Geomechanics and Engineering, *Vol. 38, No. 1 (2024) 69-77*
https://doi.org/10.12989/gae.2024.38.1.069

Prediction of tunneling parameters for ultra-large diameter slurry shield TBM in cross-river tunnels based on integrated algorithms

Shujun Xu*

China Railway 14th Bureau Group Large Shield Engineering Co., Ltd., Nanjing, 211800, China

(*Received April 1, 2024, Revised June 24, 2024, Accepted June 28, 2024*)

Abstract. The development of shield-driven cross-river tunnels in China is witnessing a notable shift towards larger diameters, longer distances, and higher water pressures due to the more complex excavation environment. Complex geological formations, such as fault and karst cavities, pose significant construction risks. Real-time adjustment of shield tunneling parameters based on parameter prediction is the key to ensuring the safety and efficiency of shield tunneling. In this study, prediction models for the torque and thrust of the cutter plate of ultra-large diameter slurry shield TBMs is established based on integrated learning algorithms, by analyzing the real data of Heyan Road cross-river tunnel. The influence of geological complexities at the excavation face, substantial burial depth, and high water level on the slurry shield tunneling parameters are considered in the models. The results reveal that the predictive models established by applying Random Forest and AdaBoost algorithms exhibit strong agreement with actual data, which indicates that the good adaptability and predictive accuracy of these two models. The models proposed in this study can be applied in the real-time prediction and adaptive adjustment of the tunneling parameters for shield tunneling under complex geological conditions.

Keywords: complex geological conditions; cross-river tunnel; integrated learning; TBM; tunneling parameters prediction; ultra-large diameter slurry shield

1. Introduction

As the rapid expansion of urban subway systems and the construction of cross-river tunnels in China, Slurry Pressure Balance Machines (SPBMs) have been extensively applied (Shi *et al.* 2023, 2024). Presently, shield tunneling is evolving towards larger diameters, longer distances, and higher water pressures (Ng *et al.* 2013, Shi *et al.* 2017, Lu *et al*. 2021, Chen *et al.* 2022, Xu *et al.* 2023), thereby significantly increasing the likelihood of encountering complex geological conditions such as mixed soft and hard layers and fault fracture zones, which poses considerable challenges to the safety of ultra-large diameter slurry shield constructions. This problem becomes even more severe for shield tunneling in karst regions. The heterogeneous distribution and varying sizes of karst formations make it difficult to accurately determine their distribution using traditional methods, which greatly increases the risks of sinking or tipping of the shield machine during construction. Therefore, self-adaptively adjusting tunneling parameters based on geological conditions is crucial for ensuring construction safety and efficiency (Bai *et al.* 2021, Shi and Wang 2021). However, traditional geological exploration methods can provide limited information, which is not enough to conduct self-adaption of tunneling parameters during construction. Machine learning methods can greatly enhance the efficiency and accuracy of real-time adjustment of tunneling parameters during construction. For example, the torque and thrust can be predicted by machine learning methods based on real-time data, and thereby adjusting the operational parameters of shield machine (Qin *et al*. 2021).

Several prediction methods of shield machine tunneling parameters have been proposed, including empirical formulas (Bruland 2000, Engineers 2007, Hassanpour *et al*. 2009, Meng *et al*. 2022, Pourhashemi *et al*. 2022, Shi *et al*. 2022), theoretical analysis (Ates *et al*. 2014, González *et al*. 2016, Meng *et al*. 2021), numerical simulation (Ring and Comulada 2018, Shi *et al*. 2019, Kim, 2021), and machine learning (Benardos and Kaliampakos 2004,; Zhao *et al*. 2007, Hassanpour *et al*. 2011, Zare Naghadehi *et al*. 2018, Koopialipoor *et al*. 2020, Mahmoodzadeh *et al*.2022). However, the empirical formula methods can only consider limited parameters and lead to lower accuracy. Theoretical analysis has difficulties in representing complex geological environments and the interaction between the slurry shield and rock. The numerical simulation methods face challenges in parameter selection and huge computation demand. In recent years, Machine learning becomes a critical way of predicting shield machine tunneling parameters due to its powerful nonlinear fitting ability. Huang *et al.* (2022) established a cutter head torque prediction model based on bidirectional long short-term memory networks. Qin *et al.* (2022) developed a cutter head torque time series prediction model using the GRU method. Song *et al.* (2019) used a fuzzy clustering algorithm to divide time series, then established a TBM thrust prediction model based on the support vector machine algorithm. Armaghani *et al.* (2019) applied three machine learning

*Corresponding author, Engineer
E-mail: cexusj2024@163.com

ISSN: 2005-307X (Print), 2092-6219 (Online)

algorithms to predict the TBM's advancement speed in different weathering zones of granite. These studies show the possibility of predicting tunneling parameters based on historical data through machine learning algorithms. However, the geological conditions of ultra-large diameter slurry shield cross-river tunnels are more complex, which makes the current methods not sufficient to guide the real-time prediction and self-adaptive adjustment of tunneling parameters.

In this study, a predictive model based on integrated learning algorithms for tunneling parameters of ultra-large diameter slurry shield cross-river tunnels is proposed, which can consider the complexity of the geological conditions at the ultra-large diameter slurry shield excavation face and the impact of high water pressure environments on tunneling parameters. The model is then validated by comparing with the real data of the Nanjing Heyan Road cross-river tunnel. The research findings can provide guidance for the safe and efficient construction of similar ultra-large diameter slurry shield cross-river tunnels.

2. Engineering background

The Heyan Road cross-river tunnel is located in Nanjing, China. The tunnel is constructed between the Yangtze River Bridge and the Yangtze River Second Bridge, approximately 7.4 km upstream from the Yangtze River Bridge and about 2.7 km downstream from the Yangtze River Second Bridge (Fig. 1). It traverses the Yangtze River, the maximum depth reaches 52.5 meters underwater, with the highest water pressure of 0.79 MPa. The tunnel has a total length of 2965 m and an excavation diameter of 15.07 m, penetrating through complex geological formations, including entire cross-section soil layers, soft-upper and hard-lower strata, fractured zones, entire cross-section rock layers, and karst areas (Fig. 2). Especially, the karst area within the tunneling region is extensive, about 487 m in length. A majority of these karst regions were explored via core drilling to ascertain the distribution of caves, with subsequent treatment using cement slurry grouting prior to excavation. However, the depiction accuracy of karst size and distribution obtained by traditional surface drilling is limited, making it difficult to accurately identify karst areas before tunneling. These varied geological formations pose substantial challenges to the safe and efficient construction employing a slurry shield machine.

The shield machine is capable to collect real-time tunneling parameters, including cutter head torque, cutter head rotation speed, and total thrust. Analysis of these tunneling parameters reveals that the slurry shield tunneling process consists of multiple cycles, each cycle comprising three phases: the empty thrust segment, rising segment, and the stable segment (Fig. 3). The empty thrust segment marks the inception of tunneling, preceding the engagement of shield with the excavation face. Subsequently, the rising segment ensues as the cutter head progressively establishes contact with the excavation face, culminating in the attainment of the preset tunneling speed. Finally, the stable

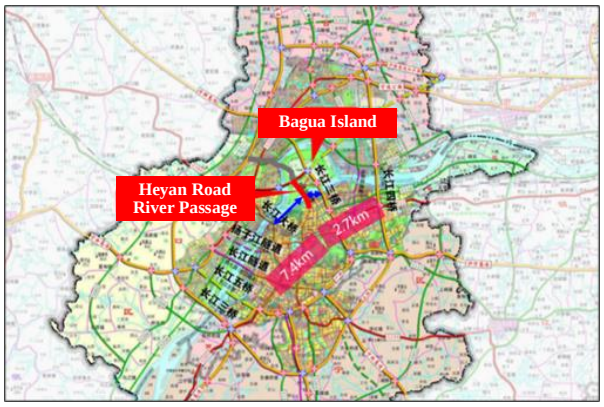

Fig. 1 Location of Heyan Road cross-river tunnel

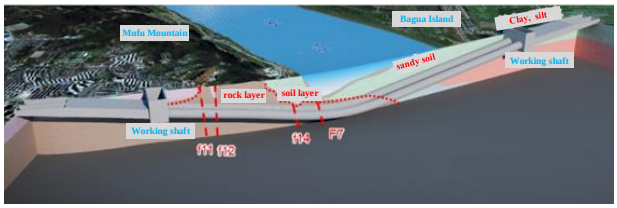

Fig. 2 Geological conditions along the tunnel

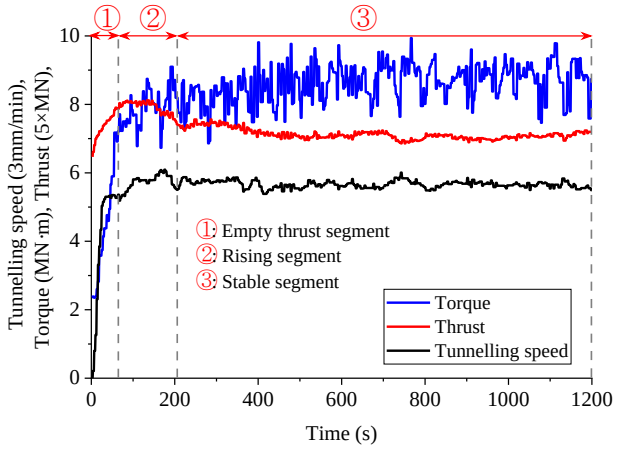

Fig. 3 Variation of tunneling parameters for a particular SPBM tunneling cycle

segment manifests wherein tunneling parameters such as speed, thrust, and torque stabilize. Particularly, the change in tunneling parameters result from the interaction between the slurry shield and the rock body and other variables. The data variation during this phase can best reflect the geological condition at the excavation face, and in the karst grouting treatment area, it can reflect the properties of the cement slurry. In contrast, the stable segment is the primary stage of safe and efficient tunneling, wherein the variation in tunneling data is notably influenced by the geological conditions of the excavation face. In light of these observations, we propose to predict the tunneling parameters of the stable segment based on the changes in tunneling parameters during the rising segment. Such predictive modeling facilitates real-time adjustments to slurry shield tunneling parameters, thereby mitigating construction risks and enhancing tunneling efficiency.

3. Machine learning algorithms

In this study, ensemble learning algorithms incorporating CART (Classification and Regression Trees), Random Forest and AdaBoost algorithms were utilized to construct a tunneling parameter prediction model suitable for large-diameter slurry shield tunnels.

3.1 CART algorithm

The CART (Salimi *et al*. 2018, Krzywinski and Altman 2017) algorithm is a widely applied decision tree algorithm. The construction of a CART decision tree involves continuously dividing the training samples (also called the root node) with the aim of making the two subsets after division as homogeneous as possible in terms of class composition. The sample set is repeatedly split until a stopping condition is met, such as when the depth of the decision tree reaches a threshold. Once the division ends, nodes are no longer split, and the terminal nodes are referred to as leaf nodes, which contain the final decision information. The key for building a CART decision tree lies in the criteria for splitting. Assuming the sample set R is divided by variable p into two subsets, $R_1(p, a) = \{x| x(p) \leq a\}$ and $R_2(p, a) = \{x| x(p) > a\}$, the optimal splitting variable and point can be determined as shown in Eq. (1).

$$\min_{p,a}[\min_{c_1} \sum_{x_n \in R_1(p,a)} (y_n - c_1)^2 + \min_{c_2} \sum_{x_n \in R_2(p,a)} (y_n - c_2)^2] \quad (1)$$

While decision trees offer the advantages of simplicity and strong interpretability, a single decision tree may lack stability, as minor variations in the data can yield vastly different decision trees. Additionally, decision tree algorithms are based on heuristic algorithms, which require optimal decisions at each node. However, this method does not ensure the return of a globally optimal decision tree. Therefore, the CART decision tree algorithm seeks to mitigate these issues by constructing multiple decision trees within an ensemble learner.

3.2 Random forest algorithm

Random Forest (Breiman 2001, Wan and Yang 2013) (RF) is an ensemble learning algorithm based on the CART decision tree, known for its high accuracy, generalization capability, and resistance to overfitting. The principle of Random Forest is depicted in Fig. 4. It starts by establishing n training subsets through the random selection of training samples and feature variables. Subsequently, n CART decision trees are built based on their respective sample subsets, each forming a regression space. Finally, Random Forest aggregates the predictions from all decision trees using Eq. (2) to arrive at the ultimate prediction result.

$$y = \frac{1}{n}\sum_{i=1}^{n} y_i(x) \quad (2)$$

In Random Forest, the method of bootstrapping is used to select n training subsets from the sample set, which enhances the diversity among CART decision trees. Moreover, the diversity among CART decision trees is further increased by randomly selecting a certain proportion

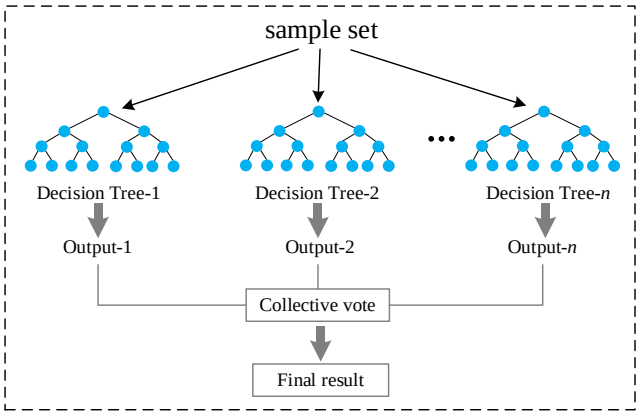

Fig. 4 Random Forest Principle

of feature variables for training of each CART decision tree, thereby improving the predictive performance of the entire ensemble model.

3.3 AdaBoost algorithm

The AdaBoost (Wang and Sun 2021) algorithm is another ensemble learning algorithm based on CART decision trees. It enhances the model's focus on samples with poor predictive outcomes by assigning weights to each training sample, thus improving the overall performance of the prediction model. Suppose a dataset $S = \{(x_i, y_i), i = 1,2,3…N\}$, where $x_i \in X$ represents the sample data, and y_i is the output value. In regression problems, the steps of the AdaBoost algorithm are as follows:

Initialize sample weights D as shown in Eq. (3)

$$\begin{cases} D^1 = (w_1^1, \ldots, w_i^1, \ldots, w_N^1) \\ w_i^1 = \dfrac{1}{N}, i = 1,2,\ldots,N \end{cases} \quad (3)$$

Train a CART decision tree with the weighted training samples to obtain a predictor $h_1(x)$. The predictor's prediction error and its weight in the final decision are calculated using Eqs. (4) and (5) respectively.

$$\varepsilon_1 = \sum_{i=1}^{N} \frac{w_i^1}{\sum_{i=1}^{N} w_i^1} |h_1(x_i) - y_i| \quad (4)$$

$$\alpha_1 = \frac{1}{2}\log\left(\frac{\varepsilon_1}{1-\varepsilon_1}\right) \quad (5)$$

Update the weight of each training sample as indicated in Eq. (6).

$$w_i^2 = w_i^1 \left(\frac{\varepsilon_1}{1-\varepsilon_1}\right)^{1-|h_1(x_i)-y_i|}, i = 1,2,\ldots,N \quad (6)$$

Repeat steps (2) and (3) until a predetermined number of cycles k is reached. Finally, aggregate the results of all predictors as shown in Eq. (7).

$$H(x) = \sum_{i=1}^{k} \alpha_i h_i(x) \quad (7)$$

4. Model evaluation methods

In the process of establishing machine learning models, there are model hyperparameters that need to be manually set, such as the number of decision trees in a random forest. In this study, the k-fold cross-validation method is used to evaluate model performance and obtain the optimal combination of hyperparameters. Meanwhile, Mean Absolute Error (MAE), Root Mean Square Error (RMSE), and R^2 score are used as metrics for evaluating model performance.

4.1 k-Fold cross-validation

In this study, the k-fold cross-validation method is employed for optimizing model hyperparameters and assessing model performance. The principle of k-fold cross-validation is illustrated in Fig. 5. The dataset D is randomly divided into k subsets. In each round of validation, k-1 subsets are used as the training set and the remaining one as the test set to conduct a performance test of the model. This process is repeated k times, and the average of the results from k rounds of testing is taken as the final cross-validation result of the model. The number of subsets k is determined by the total number of samples, typically chosen within the range of 5 to 10.

4.2 Model evaluation metrics

In order to evaluate the predictive effectiveness of the algorithm, three metrics are applied in this study: Mean Absolute Error (MAE), Root Mean Square Error (RMSE), and R^2 score. The formulas for these evaluation metrics are as follows

$$MAE = \frac{1}{n}\sum_{i=1}^{n}\left|f(x_i)-y_i\right| \tag{8}$$

$$RMSE = \sqrt{\frac{1}{n}\sum_{i=1}^{n}(f(x_i)-y_i)^2} \tag{9}$$

$$R^2 = 1-\frac{\sum_{i=1}^{n}(f(x_i)-y_i)^2}{\sum_{i=1}^{n}(\overline{f}(x_i)-y_i)^2} \tag{10}$$

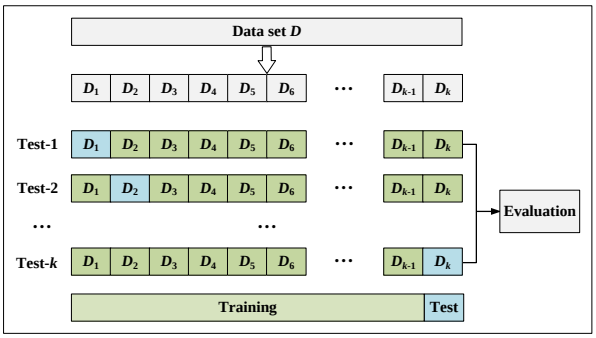

Fig. 5 Schematic of k-fold cross-validation

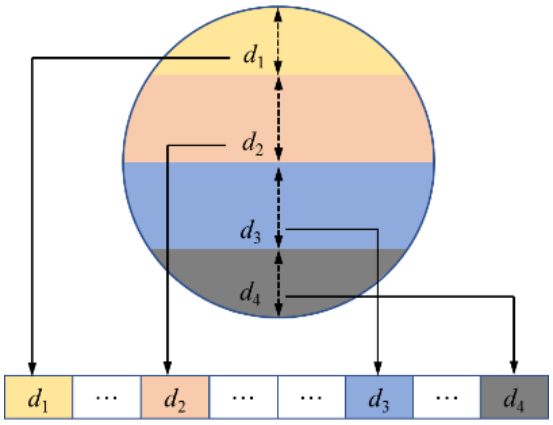

Fig. 6 Tunnel excavation surface stratigraphic information fusion method

where $f(x_i)$ is the predicted value for the sample; y_i is the actual value of the sample; n is the number of samples; and $\overline{f}(x_i)$ is the mean of the predicted values for the samples.

5. Prediction of tunneling parameters

5.1 Model input

The tunneling process of a slurry shield TBM (Tunnel Boring Machine) involves complex rock-machine interactions. Changes in tunneling parameters are closely related to the geological conditions at the tunnel face and the settings of the TBM tunneling parameters. Therefore, in this study, two crucial aspects are taken into account for the input parameters for the tunneling parameter prediction model: geological conditions and tunneling parameters, tailored to the construction characteristics of large-diameter slurry shield TBMs.

(1) Geological Conditions

The uniaxial compressive strength of the rock mass and the quartz content of the rock have been widely used in tunneling parameter prediction. However, the excavation face of a large-diameter slurry shield TBM often consists of strata with varying mechanical properties. Consequently, relying solely on the strength and mechanical properties of a single rock type proves inadequate in encapsulating the comprehensive geological characteristics of the excavation face. This study adopts a nuanced approach to characterize the properties of strata at the excavation face by considering the distribution of various strata types. As shown in Fig. 6, the thicknesses of 9 distinct strata types, along with the presence of cement slurry, at the tunnel excavation face are incorporated as input features for the model. Additionally, considering the significant impact of great tunnel depth and high water levels on slurry shield tunneling, the depth of the tunnel and groundwater level information at the excavation face are collected as feature variables.

(2) Tunneling Parameters

The average and standard deviation of mud pressure, mud inlet flow, mud outlet flow, cutter head rotation speed,

Table 1 Basic descriptive statistics of parameters

Parameter	Min.	Max.	Mean	Unit
Thickness of the silt	0	4.11	0.10	m
Thickness of the moderately dense fine sand	0	13.83	2.62	m
Thickness of the fine sand	0	11.50	1.86	m
Thickness of the silty clay with silt	0	2.40	0.03	m
Thickness of the medium coarse sand	0	7.13	0.66	m
Thickness of the gravelly medium sand	0	2.47	0.06	m
Thickness of the highly weathered breccia	0	9.36	0.63	m
Thickness of the moderately weathered breccia	0	15.07	7.60	m
Thickness of the moderately weathered limestone	0	15.07	1.40	m
Depth of the tunnel	9.73	73.69	37.06	m
Gound water level	0	45.47	10.59	m
Mud pressure	0.35	6.53	4.50	bar
Mud inlet flow	1389	3368	2480	m^3/h
Mud outlet flow	0	3878	2426	m^3/h
Total thrust	0	198465	114708	kN
Cutter head torque	0	24.23	5.60	MN·m
Cutter head rotation speed	0	1.61	1.03	rot/min
Tunneling speed	0	46.52	8.85	mm/min

tunneling speed, total thrust, and cutter head torque in the 30 seconds preceding the contact phase, are also incorporated as feature variables.

Drawing from a comprehensive dataset comprising 4582 tunneling cycles, a total of 25 input features were meticulously gathered. These encompass diverse geological information alongside tunneling parameter data, collectively constituting the feature space for the stable phase torque and thrust prediction dataset. Basic descriptive statistics of parameters is shown in Table 1.

5.2 Hyperparameter optimization

Hyperparameters, integral to machine learning models, constitute parameters that cannot be directly learned from the data, such as the minimum number of samples per leaf node in CART. These parameters wield a direct influence over the model's learning efficiency and predictive accuracy, underscoring the imperative of their meticulous evaluation and adjustment grounded in project-specific data.

In this study, 80% of the dataset (3666 tunneling cycles) was randomly selected as the training set, with the remaining 20% (916 tunneling cycles) as the test set. In the training set, grid search was employed to exhaustively explore all combinations of hyperparameters, and 6-fold cross-validation was used to evaluate the predictive performance of all hyperparameter combinations, ultimately culminating in the selection of the most effective combination. The R^2 metric was applied for model evaluation, with the ranges of hyperparameter values for each model as shown in Table 2.

Table 2 The range of hyperparameter values

Algorithms	Hyperparameters	Value range
CART	Minimum number of samples for leaf nodes	1~5
	Minimum number of samples that can be split	2~5
Random forest	Number of decision trees	100~200
	Minimum number of samples for leaf nodes	1~5
	Minimum number of samples that can be split	2~5
AdaBoost	Number of decision trees	50~200
	Learning rate	0.6~2

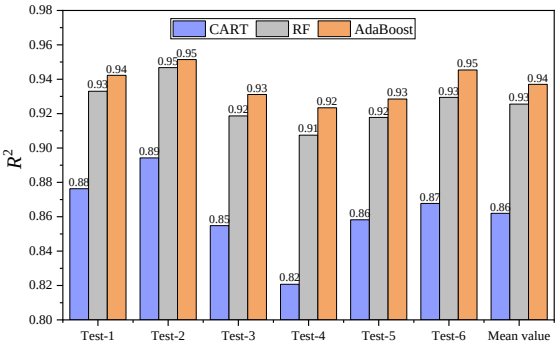

Fig. 7 Cross-validation results of torque prediction under different algorithms

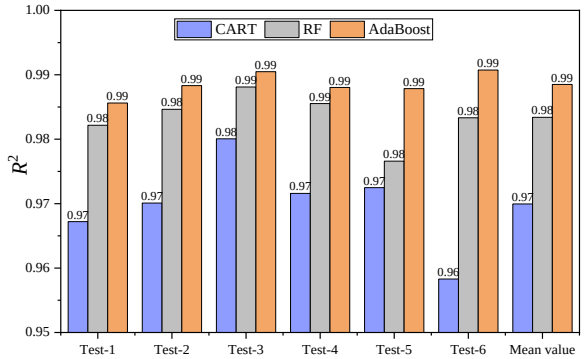

Fig. 8 Cross-validation results of thrust prediction under different algorithms

In the context of torque prediction, the optimal cross-validation results for the three types of algorithms are depicted in Fig. 7. The average 6-fold cross-validation scores for CART, Random Forest, and AdaBoost models are respectively 0.86, 0.93, and 0.94. It is evident that the accuracy of the CART model notably lags behind that of Random Forest and AdaBoost. The results from six tests of the three algorithms reveals that the CART algorithm exhibits considerable fluctuation in prediction accuracy, ranging from 0.82 to 0.89, whereas Random Forest and AdaBoost models show less variability in prediction

Table 3 Optimal hyperparameter combinations for different algorithms

Algorithms	Hyperparameters	Torque Prediction	Thrust Prediction
CART	Minimum number of samples for leaf nodes	4	4
	Minimum number of samples that can be split	4	3
Random forest	Number of decision trees	150	110
	Minimum number of samples for leaf nodes	1	1
	Minimum number of samples that can be split	2	3
AdaBoost	Number of decision trees	150	190
	Learning rate	1.4	1.8

Table 4 Comparison of the accuracy for torque on the training and test sets for three algorithms

Algorithms	R^2 on the train set	R^2 on the test set
CART	0.86	0.896
RF	0.93	0.936
AdaBoost	0.94	0.943

accuracy across different tests. The optimal cross-validation results for the thrust prediction are shown in Fig. 8: The average 6-fold cross-validation scores for CART, Random Forest, and AdaBoost models are respectively 0.97, 0.98, and 0.99, indicating that all three algorithms achieve high accuracy in thrust prediction.

Grid search and 6-fold cross-validation were then used to optimize the hyperparameters for the torque and thrust prediction models. The resulting optimal hyperparameter combinations are meticulously presented in Table 3.

5.3 Model application

In this section, the prediction models for torque and thrust are established based on the CART, Random Forest, and AdaBoost algorithms. The 4583×23 feature matrix obtained in Section 5.1 is served as the input data, and 80% of the data was randomly selected as the training set based on the optimal hyperparameter combinations and training set data from Section 5.2. Real-time torque value of the stable phase for that tunneling cycle can be derived from the models by inputting the geological data and the average and standard deviation of the tunneling parameters in the 30 seconds before the contact phase into the model. In order to further evaluate the predictive models, the remaining 20% of the data was used as the test set to assess the predictive performance of the models.

The comparison of prediction accuracy for torque and thrust on the training and test sets for the CART, RF, and AdaBoost algorithms is shown in Tables 4 and 5. It can be observed that the accuracy of these three algorithms on the training and test sets is relatively close, indicating good

Table 5 Comparison of the accuracy for thrust on the training and test sets for three algorithms

Algorithms	R^2 on the train set	R^2 on the test set
CART	0.97	0.973
RF	0.98	0.986
AdaBoost	0.99	0.987

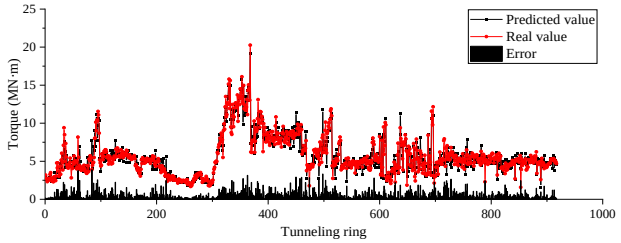

(a) CART

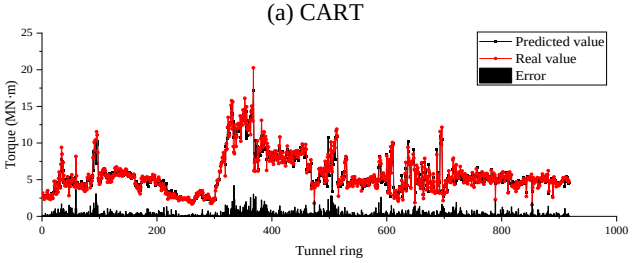

(b) RF

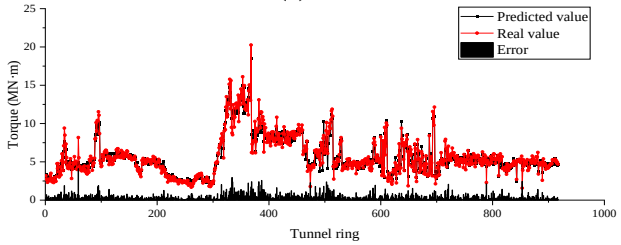

(c) AdaBoost

Fig. 9 Torque prediction results

model training performance without overfitting or underfitting issues.

The torque prediction results on the test set generated by models established using CART, Random Forest (RF), and AdaBoost algorithms are shown in Fig. 9. It was observed that the torque predictions at the stable phase by the RF and AdaBoost algorithms, were closer to the actual measurements with smaller absolute errors. Upon comprehensive evaluation of the predictive performance across these three algorithms, it emerged that the R_2 values for CART, Random Forest, and AdaBoost amounted to 0.896, 0.936, and 0.943, respectively. The Mean Absolute Errors (MAE) for these algorithms were 0.588 MN·m, 0.433 MN·m, and 0.431 MN·m, respectively. This indicates that the CART algorithm yielded the lowest accuracy in torque prediction, followed by Random Forest, while AdaBoost achieving the highest accuracy.

The thrust prediction results on the test set for the three algorithms are shown in Fig. 11. The R^2 values for CART, Random Forest, and AdaBoost were 0.973, 0.986, and 0.987, respectively. Additionally, the MAEs were 2.472 MN·m for CART, 1.775 MN·m for Random Forest, and 1.733 MN·m for AdaBoost, while the Root Mean Square

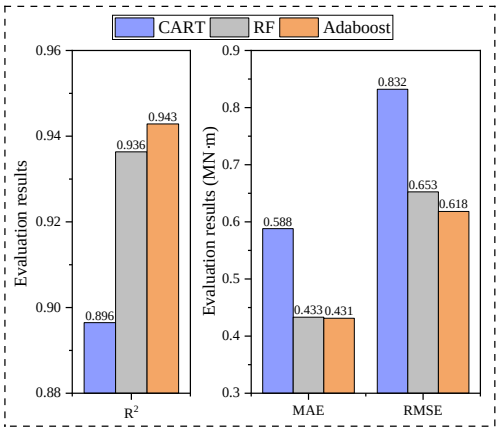

Fig. 10 Evaluation of three types of algorithms on torque prediction performance

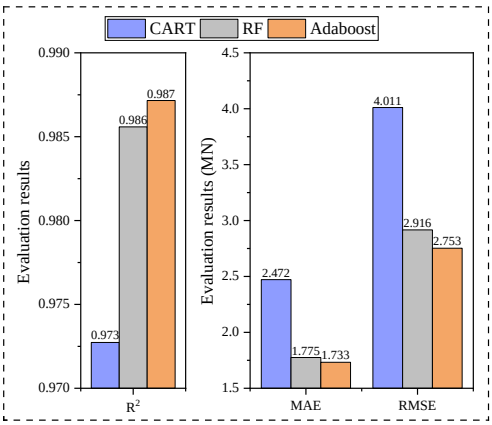

Fig. 12 Evaluation of three types of algorithms on thrust prediction performance

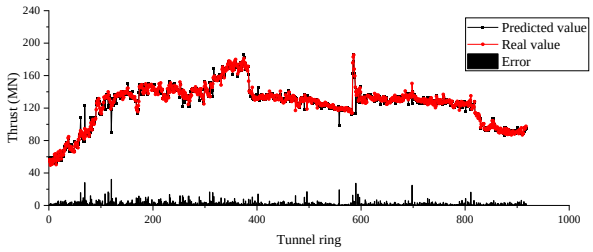

(a) CART

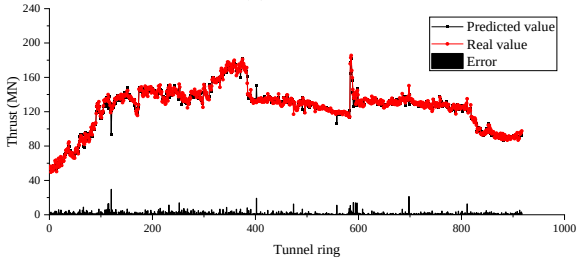

(b) RF

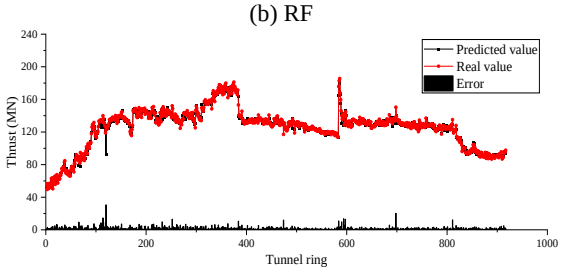

(c) AdaBoost

Fig. 11 Thrust prediction results

Errors (RMSEs) were 4.011 MN·m for CART, 2.916 MN·m for Random Forest, and 2.753 MN·m for AdaBoost. These results indicate that the thrust predictions from the ensemble learning-based Random Forest and AdaBoost models were closest to the actual values, exhibiting diminutive prediction errors.

A further comparison of the actual and predicted values of torque and thrust for a specific tunneling cycle (Fig. 13) demonstrated that the predictions obtained from the ensemble learning-based Random Forest and AdaBoost models are close to the original trend curves. The models based on the ensemble learning-based Random Forest and AdaBoost algorithms can predict the real-time tunneling parameters well.

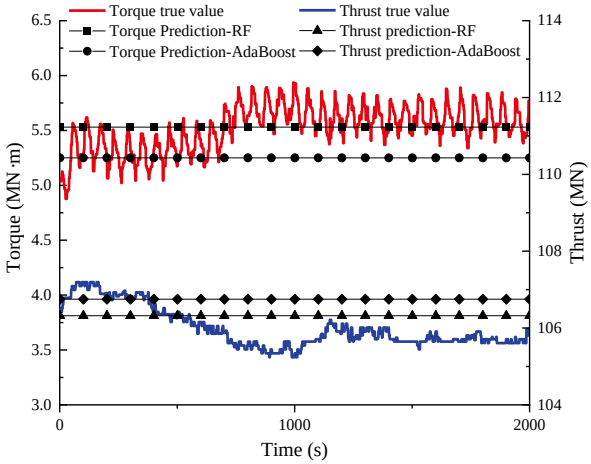

Fig. 13 Comparison of real and predicted values of cutter torque and total thrust of a tunneling cycle

6. Conclusions

In order to address the challenges of adaptive and safe construction of ultra-large diameter slurry shield TBMs in cross-river tunnels, a tunneling parameter prediction model based on the ensemble learning algorithms for ultra-large diameter slurry shield TBMs in cross-river tunnels were proposed in this study. The impacts of geological complexity at the excavation face, deep burial, and high water level on the slurry shield TBM's tunneling parameters were considered in the models.

Through rigorous training of the constructed Random Forest and AdaBoost models, the framework facilitates real-time prediction of shield cutter head torque and thrust. Specifically, in the prediction of cutter head torque, the R^2 values for Random Forest and AdaBoost were 0.936 and 0.943, respectively. In the prediction of thrust, the R^2 values for Random Forest and AdaBoost were 0.986 and 0.987, respectively. Thereby it provides data support for the adaptive operational parameters of the slurry shield TBM, thus significantly enhancing the efficacy of real-time prediction and adaptive adjustment of tunneling parameters for ultra-large diameter slurry shield TBM in cross-river tunnels

7. Limitations

Although the Random Forest and AdaBoost algorithms handle high-dimensional data well and exhibit high predictive performance, their efficiency can be affected by the size and complexity of the data. Therefore, in this study, the lack of further input feature compression may impact the training efficiency of the predictive models.

References

Armaghani, D.J., Koopialipoor, M., Marto, A. and Yagiz, S. (2019), "Application of several optimization techniques for estimating TBM advance rate in granitic rocks", *J. Rock Mech. Geotech. Eng.*, **11**(4), 779-789. https://doi.org/10.1016/j.jrmge.2019.01.002.

Ates, U., Bilgin, N. and Copur, H. (2014), "Estimating torque, thrust and other design parameters of different type TBMs with some criticism to TBMs used in Turkish tunneling projects", *Tunn. Undergr. Sp. Tech.*, **40**, 46-63. https://doi.org/10.1016/j.tust.2013. 09.004.

Bai, X., Cheng, W., Ong Dominic, E.L. and Li, G. (2021), "Evaluation of geological conditions and clogging of tunneling using machine learning", *Geomech. Eng.*, **25**(1), 59-73. https://doi.org/10.12989/gae.2021.25.1.059.

Benardos, A.G. and Kaliampakos, D.C. (2004), "Modelling TBM performance with artificial neural networks", *Tunn. Undergr. Sp. Tech.*, **19**(6), 597-605. https://doi.org/10.1016/j.tust.2004.02.128.

Breiman, L. (2001), "Random Forests", *Machine Learning*, **45**(1), 5-32. https://doi.org/10.1023/a:1010933404324.

Bruland, A. (2000), Hard rock tunnel boring, Ph.D. Dissertation; Norwegian University of Science and Technology, Trondheim, Norway.

Chen, R.P., Song, X., Meng, F.Y., Wu, H.N. and Lin, X.T. (2022), "Analytical approach to predict tunneling-induced subsurface settlement in sand considering soil arching effect", C*omput. Geotech.*, **141**, 104492. https://doi.org/10.1016/j.compgeo.2021.104492.

Engineers, J.S.O.C. (2007), *Standard Specifications for Tunneling: Shield Tunnel,* Japan Society of Civil Engineers, Tokyo, Japan.

González, C., Arroyo, M. and Gens, A. (2016), "Thrust and torque components on mixed-face EPB drives", *Tunn. Undergr. Sp. Tech.*, **57**(8), 47-54. https://doi.org/10.1016/j.tust.2016.01.037.

Hassanpour, J., Rostami, J., Khamehchiyan, M. and Bruland, A. (2009), "Developing new equations for TBM performance prediction in carbonate-argillaceous rocks: a case history of Nowsood water conveyance tunnel", *Geomech. Geoeng.*, **4**(4), 287-297. https://doi.org/10.1080/17486020903174303.

Hassanpour, J., Rostami, J. and Zhao, J. (2011), "A new hard rock TBM performance prediction model for project planning", *Tunn. Undergr. Sp. Tech.*, **26**(5), 595-603. https://doi.org/10.1016/ j.tust.2011.04.004.

Huang, X., Zhang, Q., Liu, Q., Liu, X., Liu, B., Wang, J. and Yin, X. (2022), "A real-time prediction method for tunnel boring machine cutter-head torque using bidirectional long short-term memory networks optimized by multi-algorithm", *J. Rock Mech. Geotech. Eng.*, 247272490. https://doi.org/10.1016/j.jrmge. 2021. 11. 008.

Krzywinski, M., and Altman, N. (2017), "Classification and regression trees", *Nature Methods,* **14**, 757-758. https://doi.org/10.1038/nmeth.4370.

Kim, D. (2021), "Large deformation finite element analyses in TBM tunnel excavation: CEL and auto-remeshing approach", *Tunn. Undergr. Sp. Tech.*, **116**(10), 104081. https://doi.org/10.1016/ j.tust.2021.104081.

Koopialipoor, M., Fahimifar, A., Ghaleini, E.N., Momenzadeh, M. and Armaghani, D.J. (2020), "Development of a new hybrid ANN for solving a geotechnical problem related to tunnel boring machine performance", *Eng. with Comput.*, **36**(1), 345-357. https://doi.org/10.1007/s00366-019-00701-8.

Lu, J., Gong, Q., Yin, L. and Zhou, X. (2021), "Study on the tunneling response of TBM in stressed granite rock mass in Yinhan Water Conveyance tunnel", *Tunn. Undergr. Sp. Tech.*, **118**(3), 104197. https://doi.org/10.1016/j.tust.2021.104197.

Mahmoodzadeh, A., Nejati Hamid, R., Ibrahim Hawkar, H., Ali Hunar Farid, H., Mohammed Adil, H., Rashidi, S. and Majeed Mohammed, K. (2022), "Several models for tunnel boring machine performance prediction based on machine learning", *Geomech. Eng.*, **30**(1), 75-91. https://doi.org/10.12989/gae.2022.30.1.075.

Meng, F.Y., Chen, R.P., Xu, Y., Wu, K., Wu, H.N. and Liu, Y. (2022), "Contributions to responses of existing tunnel subjected to nearby excavation: a review", *Tunn. Undergr. Sp. Tech.*, **119**, 104195. https://doi.org/ 10.1016/j.tust.2021.104195.

Meng, F.Y., Chen, R.P., Liu, S.L. and Wu, H.N. (2021), "Centrifuge modeling of ground and tunnel responses to nearby excavation in soft soil", *J. Geotech. Geoenviron. Eng.*, **147**(3), 04020178. https://doi.org/10.1061/(ASCE)GT.1943-5606.0002473.

Ng, C.W.W., Shi, J.W. and Hong, Y. (2013), "Three-dimensional centrifuge modelling of basement excavation effects on an existing tunnel in dry sand", *Can. Geotech. J.*, **50**(8), 874-888. https://doi.org/10.1139/cgj-2012-0423.

Pourhashemi, S.M., Ahangari, K., Hassanpour, J. and Eftekhari, S.M. (2022), "TBM performance analysis in very strong and massive rocks; case study: Kerman water conveyance tunnel project, Iran", *Geomech. Geoeng.*, **17**(4), 1110-1122. https://doi.org/ 10.1080/17486025.2021.1912410.

Qin, C., Shi, G., Tao, J., Yu, H., Jin, Y., Lei, J. and Liu, C. (2021), "Precise cutterhead torque prediction for shield tunneling machines using a novel hybrid deep neural network", *Mech. Syst. Signal Pr.*, **151**(4), 107386. https://doi.org/10.1016/j.ymssp.2020. 107386.

Qin, C., Shi, G., Tao, J., Yu, H., Jin, Y., Xiao, D., Zhang, Z. and Liu, C. (2022), "An adaptive hierarchical decomposition-based method for multi-step cutterhead torque forecast of shield machine", *Mech. Syst. Signal Pr.*, **175**(8), 109148. https://doi.org/ 10.1016/j.ymssp.2022.109148.

Ring, B. and Comulada, M. (2018), "Practical numerical simulation of the effect of TBM process pressures on soil displacements through 3D shift iteration", *Undergr. Sp.*, **3**(4), 297-309. https://doi.org/10.1016/j.undsp. 2018.09.003.

Salimi, A., Rostami, J., Moormann, C. and Hassanpour, J. (2018), "Examining feasibility of developing a rock mass classification for hard rock TBM application using non-linear regression, regression tree and generic programming", *Geotech. Geol. Eng.*, **36**(2), 1145-1159. https://doi.org/10.1007/s10706-017-0380-z.

Shi, J.W., Chen, Y.H., Kong, G.Q., Lu, H., Chen, G. and Shi C. (2024), "Deformation mechanisms of an existing pipeline due to progressively passive instability of tunnel face: physical and numerical investigations", *Tunn. Undergr. Sp. Tech.*, **150**, 105822. https://doi.org/10.1016/j.tust.2024.105822.

Shi, J.W., Wang, J.P., Chen Y.H., Shi, C., Lu, H., Ma, S.K. and Fan, Y.B. (2023), "Physical modeling of the influence of tunnel active face instability on existing pipelines", *Tunn. Undergr. Sp. Tech.*, **140**, 105281. https://doi.org/ 10.1016/j.tust.2023.105281.

Shi, J.W., Chen, Y.H., Lu, H., Ma, S.K. and Ng, C.W.W. (2022), "Centrifuge modeling of the influence of joint stiffness on pipeline response to underneath tunnel excavation", *Can. Geotech. J.*, **59**(9), 1568-1586. https://doi.org/10.1139/cgj-2020-03601.

Shi, J., Fu, Z.Z. and Guo, W.L. (2019), "Investigation of geometric effects on three-dimensional tunnel deformation mechanisms due to basement excavation", *Comput. Geotech.*, **106**, 108-116. https://doi.org/ 10.1016/j.compgeo.2018.10.019.

Shi, J., Zhang, X., Chen, L. and Chen, L. (2017), "Numerical investigation of pipeline responses to tunneling-induced ground settlements in clay", *Soil Mech. Found. Eng.*, **54**, 303-309. https://doi.org/10.1007/s11204-017-9473-1.

Shi, C. and Wang, Y. (2021), "Development of Subsurface Geological Cross-section from limited site-specific boreholes and prior geological knowledge using iterative convolution XGBoost", *J. Geotech. Geoenviron. Eng.*, **147**(9), 04021082. https://doi.org/10.1061/(ASCE)GT. 1943-5606. 0002583.

Song, X., Shi, M., Wu, J. and Sun, W. (2019), "A new fuzzy c-means clustering-based time series segmentation approach and its application on tunnel boring machine analysis", *Mech. Syst. Signal Pr.*, **133**(11), 106279. https://doi.org/10.1016/j.ymssp.2019. 106279.

Wan, S. and Yang, H. (2013), "Comparison among methods of ensemble learning" *Proceedings of the 2013 International Symposium on Biometrics and Security Technologies*, Chengdu, China, July.

Wang, W. and Sun, D. (2021), "The improved AdaBoost algorithms for imbalanced data classification", *Inform. Sci.*, **563**(7), 358-374. https://doi.org/10.1016/j.ins.2021.03.042.

Xu, D., Wang, Y., Huang, J., Liu, S., Xu, S. and Zhou, K. (2023), "Prediction of geology condition for slurry pressure balanced shield tunnel with super-large diameter by machine learning algorithms", *Tunn. Undergr. Sp. Tech.*, **131**(1), 104852. https://doi.org/10.1016/j.tust.2022.104852.

Zare Naghadehi, M., Samaei, M., Ranjbarnia, M. and Nourani, V. (2018), "State-of-the-art predictive modeling of TBM performance in changing geological conditions through gene expression programming", *Measurement*, **126**, 46-57. https://doi.org/10.1016/j.measurement.2018. 05.049.

Zhao, Z., Gong, Q., Zhang, Y. and Zhao, J. (2007), "Prediction model of tunnel boring machine performance by ensemble neural networks", *Geomech. Geoeng.*, **2**(2), 123-128. https://doi.org/10.1080/ 17486020701377140.

GC